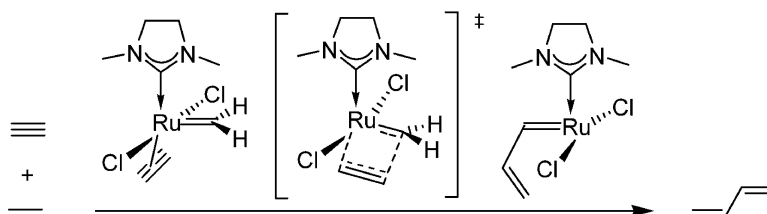


Mechanism of Enyne Metathesis Catalyzed by Grubbs Ruthenium–Carbene Complexes: A DFT Study

Jrg J. Lippstreu, and Bernd F. Straub

J. Am. Chem. Soc., **2005**, 127 (20), 7444-7457 • DOI: 10.1021/ja042622g • Publication Date (Web): 27 April 2005

Downloaded from <http://pubs.acs.org> on March 25, 2009



More About This Article

Additional resources and features associated with this article are available within the HTML version:

- Supporting Information
- Links to the 20 articles that cite this article, as of the time of this article download
- Access to high resolution figures
- Links to articles and content related to this article
- Copyright permission to reproduce figures and/or text from this article

[View the Full Text HTML](#)



Mechanism of Enyne Metathesis Catalyzed by Grubbs Ruthenium–Carbene Complexes: A DFT Study

Jörg J. Lippstreu and Bernd F. Straub*

Contribution from the Department Chemie und Biochemie der Ludwig-Maximilians-Universität München, Butenandtstr. 5-13 (Haus F), D-81377 München, Germany

Received December 8, 2004; E-mail: Bernd.F.Straub@cup.uni-muenchen.de

Abstract: The complete catalytic cycle of the reaction of alkenes and alkynes to dienes by Grubbs ruthenium carbene complexes has been modeled at the B3LYP/LACV3P**+//B3LYP/LACVP* level of theory. The core structures of the substrates and the catalyst were used as models, namely, ethene, ethyne, hept-1-en-6-yne, $(\text{Me}_3\text{P})_2\text{Cl}_2\text{Ru}=\text{CH}_2$, and $[\text{C}_2\text{H}_4(\text{NMe})_2\text{C}](\text{Me}_3\text{P})\text{Cl}_2\text{Ru}=\text{CH}_2$. Insight into the electronically most preferred mechanistic pathways was gained for both intermolecular as well as for intramolecular enyne metathesis. Alkene metathesis is predicted to proceed fast and reversible, while the insertion of the alkyne substrate is slower, irreversible, and kinetically regioselectivity determining. Ruthenacyclobut-2-ene structures do not exist as local minima in the catalytic cycle. Instead, vinylcarbene complexes are formed directly. The alkyne insertion step and the cycloreversion of 2-vinyl ruthenacyclobutanes feature comparable predicted overall barriers in intermolecular enyne metathesis. For intramolecular enyne metathesis, a noncyclic alkene fragment of the enyne substrate is first incorporated into the Grubbs catalyst by an alkene metathesis reaction. The subsequent insertion of the alkyne fragment then proceeds intramolecularly. Alkene association, cycloaddition, and cycloreversion to the diene product complex close the catalytic cycle. Rate enhancement by an ethene atmosphere (Mori's conditions) originates from a constantly higher overall alkene concentration that is necessary for the rate-limiting $[2 + 2]$ cycloreversion step to the diene product complex.

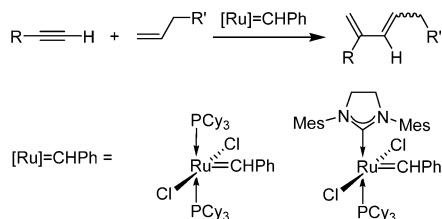
Introduction

Ruthenium carbene complexes have been investigated as catalysts for numerous alkene transformation reactions.¹ Cross metathesis (CM),² ring-closing metathesis (RCM), acyclic diene metathesis (ADMET), and ring-opening metathesis polymerization (ROMP) reflect the diversity of alkene metathesis reactions. Their mechanisms are based on the facile $[2 + 2]$ cycloaddition of an alkene and a 14 valence electron ruthenium carbene intermediate to a ruthenacyclobutane complex and its cycloreversion.³ The mechanism has been investigated thoroughly both experimentally⁴ as well as theoretically.^{4c,5} A further application for Grubbs ruthenium carbene complexes was realized in the enyne metathesis reaction (enyne bond rearrangement).⁶ Therein, an alkene and an alkyne yield a 1,3-diene product. Both intramolecular^{6,7} as well as intermolecular^{6,8} enyne

metathesis reactions have been reported, both with first-⁹ and second-generation Grubbs catalysts.¹⁰ Formally, the two methylene fragments of the alkene add across the alkyne triple bond,

- (1) (a) Trnka, T. M.; Grubbs, R. H. *Acc. Chem. Res.* **2001**, *34*, 18. (b) Schuster, M.; Blechert, S. *Chem. Z.* **2001**, *35*, 24. (c) Roy, R.; Das, S. K. *Chem. Commun.* **2000**, 519. (d) Fürstner, A. *Angew. Chem.* **2000**, *112*, 3140; *Angew. Chem., Int. Ed.* **2000**, *39*, 3012. (e) Grubbs, R. H.; Chang, S. *Tetrahedron* **1998**, *54*, 4413. (f) Schuster, M.; Blechert, S. *Angew. Chem., Int. Ed.* **1997**, *109*, 2124; *Angew. Chem., Int. Ed. Engl.* **1997**, *36*, 2036.
- (2) Connon, S. J.; Blechert, S. *Angew. Chem.* **2003**, *115*, 1944; *Angew. Chem., Int. Ed.* **2003**, *42*, 1900.
- (3) Hérisson, J.-L.; Chauvin, Y. *Makromol. Chem.* **1971**, *141*, 161.
- (4) (a) Hinderling, C.; Adlhart, C.; Chen, P. *Angew. Chem.* **1998**, *110*, 2831; *Angew. Chem., Int. Ed.* **1998**, *37*, 2685. (b) Adlhart, C.; Volland, M. A. O.; Hofmann, P.; Chen, P. *Helv. Chim. Acta* **2000**, *83*, 3306. (c) Adlhart, C.; Hinderling, C.; Baumann, H.; Chen, P. *J. Am. Chem. Soc.* **2000**, *122*, 8204. (d) Sanford, M. S.; Ulman, M.; Grubbs, R. H. *J. Am. Chem. Soc.* **2001**, *123*, 749. (e) Sanford, M. S.; Love, J. A.; Grubbs, R. H. *J. Am. Chem. Soc.* **2001**, *123*, 6543. (f) Volland, M. A. O.; Adlhart, C.; Kiener, C. A.; Chen, P.; Hofmann, P. *Chem. Eur. J.* **2001**, *7*, 4621.
- (5) (a) Aagaard, O. M.; Meier, R. J.; Buda. *J. Am. Chem. Soc.* **1998**, *120*, 7174. (b) Hansen, S. M.; Rominger, F.; Metz, M.; Hofmann, P. *Chem. Eur. J.* **1999**, *5*, 557. (c) Meier, R. J.; Aagaard, O. M.; Buda, F. *J. Mol. Catal. A* **2000**, *160*, 189. (d) Vyboishikov, S. F.; Bühl, M.; Thiel, W. *Chem. Eur. J.* **2002**, *8*, 3962. (e) Cavallo, L. *J. Am. Chem. Soc.* **2002**, *124*, 8965. (f) Adlhart, C.; Chen, P. *Angew. Chem.* **2002**, *114*, 4668; *Angew. Chem., Int. Ed.* **2002**, *41*, 4484. (g) Fomine, S.; Vargas, S. M.; Tlenkopatchev, M. A. *Organometallics* **2003**, *22*, 93. (h) Bernardi, F.; Bottoni, A.; Miscione, G. P. *Organometallics* **2003**, *22*, 940. (i) Adlhart, C.; Chen, P. *J. Am. Chem. Soc.* **2004**, *126*, 3496. (j) Suresh, C. H.; Koga, N. *Organometallics* **2004**, *23*, 76. (k) Burdett, K. A.; Harris, L. D.; Margl, P.; Maughon, B. R.; Mokhtar-Zadeh, T.; Saucier, P. C.; Wasserman, E. P. *Organometallics* **2004**, *23*, 2027. (l) Costabile, C.; Cavallo, L. *J. Am. Chem. Soc.* **2004**, *126*, 9592. (m) van Rensburg, W. J.; Steynberg, P. J.; Meyer, W. H.; Kirk, M. M.; Grant S. Forman, G. S. *J. Am. Chem. Soc.* **2004**, *126*, 14332.
- (6) For reviews, see (a) Diver, S. T.; Giessert, A. J. *Chem. Rev.* **2004**, *104*, 1317. (b) Diver, S. T.; Giessert, A. J. *Synthesis* **2004**, 466. (c) Poulsen, C. S.; Madsen, R. *Synthesis* **2003**, 1. (d) Mori, M. *Top. Organomet. Chem.* **1998**, *1*, 133.
- (7) (a) Kinoshita, A.; Mori, M. *Synlett* **1994**, 1020. (b) Mori, M.; Kitamura, T.; Sakakibara, N.; Sato, Y. *Org. Lett.* **2000**, *2*, 543. (c) Mori, M.; Kitamura, T.; Sato, Y. *Synthesis* **2001**, 654. (d) Poulsen, C. S.; Madsen, R. *J. Org. Chem.* **2002**, *67*, 4441. For further examples, see review 6a.
- (8) (a) Stragies, R.; Schuster, M.; Blechert, S. *Angew. Chem.* **1997**, *109*, 2628; *Angew. Chem., Int. Ed. Engl.* **1997**, *36*, 2518. (b) Kulkarni, A. A.; Diver, S. T. *J. Am. Chem. Soc.* **2004**, *126*, 8110. (c) Kulkarni, A. A.; Diver, S. T. *Org. Lett.* **2003**, *5*, 3463. (d) Giessert, A. J.; Brazis, N. J.; Diver, S. T. *Org. Lett.* **2003**, *5*, 3819. (e) Kim, M.; Park, S.; Maifeld, S. V.; Lee, D. J. *Am. Chem. Soc.* **2004**, *126*, 10242. For further examples, see review 6a.
- (9) (a) Nguyen, S. T.; Johnson, L. K.; Grubbs, R. H. *J. Am. Chem. Soc.* **1992**, *114*, 3974. (b) Wu, Z.; Benedicto, A. D.; Grubbs, R. H. *Macromolecules* **1993**, *26*, 4975. (c) Nguyen, S. T.; Ziller, J. W.; Grubbs, R. H. *J. Am. Chem. Soc.* **1993**, *115*, 9858. (d) Schwab, P.; Grubbs, R. H.; Ziller, J. W. *J. Am. Chem. Soc.* **1996**, *118*, 100. (e) Schwab, P.; France, M. B.; Ziller, J. W.; Grubbs, R. H. *Angew. Chem.* **1995**, *107*, 2179; *Angew. Chem., Int. Ed. Engl.* **1995**, *34*, 2039.

converting it into an sp^2 – sp^2 single bond of the conjugated diene product.



While B. M. Trost and co-workers have successfully studied the mechanism of the palladium-catalyzed enyne metathesis reaction,¹¹ the mechanism of the ruthenium carbene analogue has yet to be unraveled.¹² Vinylcarbene ruthenium complexes are likely intermediates of the reaction. The closest structurally isolated complexes are η^3 -vinylcarbene ruthenium complexes.¹³ However, the latter have been characterized only with sterically demanding alkyne substrates. These η^3 -vinylcarbene ruthenium complexes display a high thermal stability, but their catalytic inactivity does not support an important role as catalytic intermediate.¹³ Ruthenacyclobut-2-ene derivatives are commonly assumed as intermediates but have neither been isolated nor even been detected spectroscopically. The mechanistic origin of the beneficial effect of an ethene atmosphere (Mori's conditions) toward increasing selectivity and rate enhancement in the enyne metathesis reaction has also to be addressed.¹⁴ The questions of the identity of the catalyst resting state, the rate-limiting step, and the selectivity-determining step also have yet to be unraveled. In this DFT study, we report on the complete mechanistic cycle for the intermolecular enyne metathesis catalyzed by Grubbs complexes. Furthermore, intramolecular enyne metathesis is modeled for second-generation ruthenium carbene catalysts.

Computational Details

The B3LYP/LACV3P**+/B3LYP/LACVP* level of theory¹⁵ as implemented in the Jaguar 4.1 quantum chemistry program package¹⁶ has been utilized throughout this study. For N, C, P, Cl, and H, the 6-31G* basis set of Pople and co-workers was used for geometry

optimizations.¹⁷ For ruthenium, a Hay-Wadt small effective core potential replaces the 28 innermost core electrons.¹⁸ The basis set on ruthenium has double- ζ quality for geometry optimization (contraction scheme {331/311/31}) and triple- ζ quality for single-point energy calculations (contraction scheme {3211/2111/2111}). Full geometry optimizations and analytical vibrational frequency calculations have been performed for all model compounds on the B3LYP/LACVP* level of theory. Exactly zero imaginary vibrations characterize stationary points; transition structures are characterized by exactly one imaginary vibration. Visual inspection of imaginary vibrations was performed with the Molden program package¹⁹ and geometry optimizations from slightly distorted transition-state structures ensured the assignment of the two corresponding local minima. Single-point energies were computed analytically with the LACV3P**+ basis set, which is characterized by the 6-311G**+ basis set for main group elements^{17,20} and by a diffuse d function for ruthenium (coefficient 0.042). A self-consistent field energy convergence threshold of 1×10^{-5} a.u. was applied for single-point energy calculations. The Gibbs free energies G refer to 298.15 K and 1 atm and are based on unscaled molecular vibrations and ideal gas-phase conditions. Overall free activation energies of investigated catalytic cycles are based on Gibbs free-energy differences between the rate-limiting transition-state structure and the catalyst resting state. Free activation energies of single steps are based on Gibbs free energy differences between the respective transition state structure and the originating local minimum. In this study, the word “barrier” is used sometimes as a synonym for Gibbs free activation energy.

The coordination and dissociation of alkene, alkyne, and phosphane ligands at ruthenium fragments proceed without intrinsic barriers. Scans of the energy hypersurface were performed to ensure the nonexistence of transition states for these processes. Dotted lines in energy diagrams indicate the lack of enthalpic barriers for association or dissociation reactions and an entropic contribution to the Gibbs free activation barrier of presumably 20–30 kJ mol⁻¹.

The computation of the pathways for the intramolecular enyne metathesis reaction do not include rotation steps around carbon–carbon single bonds, as indicated by undulatory lines in energy diagrams.

The accuracy of the comparison of computed relative energies of ruthenium model complexes with relative energies of experimental “real” ruthenium complexes is influenced by the gas-phase restriction of the model complexes, the steric simplification of the NHC ligand and the substrate, and the intrinsic inaccuracy of the functionals and basis sets. As a result, the predicted overall barriers appear to be slightly overestimated compared to the experimental reaction conditions. The computed relative free energies of 14 valence electron ruthenium complexes with a lower coordination number feature presumably the largest deviations, since entropic effects of the solvation of free ligands and substrates are proposed to have a considerable influence.²¹ The used quantum-chemical methodology was validated both structurally and energetically (see Supporting material).

Discussion

We were mainly interested in the electronic preferences of the catalyst and the substrates on the mechanism of the title reaction. Therefore, we neglected steric effects and influences

- (10) (a) Weskamp, T.; Schattenmann, W. C.; Spiegler, M.; Herrmann, W. A. *Angew. Chem.* **1998**, *110*, 2631; *Angew. Chem., Int. Ed.* **1998**, *37*, 2490. (b) Huang, J.; Stevens, E. D.; Nolan, S. P.; Petersen, J. L.; *J. Am. Chem. Soc.* **1999**, *121*, 2674. (c) Weskamp, T.; Kohl, F. J.; Hieringer, W.; Gleich, D.; Herrmann, W. A.; *Angew. Chem.* **1999**, *111*, 2573; *Angew. Chem., Int. Ed.* **1999**, *38*, 2416. (d) Scholl, M.; Trnka, T. M.; Morgan, J. P.; Grubbs, R. H. *Tetrahedron Lett.* **1999**, *40*, 2247. (e) Scholl, M.; Ding, S.; Lee, C. W.; Grubbs, R. H. *Org. Lett.* **1999**, *1*, 953.
- (11) (a) Trost, B. M.; Tanoury, G. J. *J. Am. Chem. Soc.* **1988**, *110*, 1636. (b) Trost, B. M.; Trost, M. K. *Tetrahedron Lett.* **1991**, *32*, 3647. (c) Trost, B. M.; Trost, M. K. *J. Am. Chem. Soc.* **1991**, *113*, 1850. (d) Trost, B. M.; Chang, V. K. *Synthesis* **1993**, 824. (e) Trost, B. M.; Yanai, M.; Hoogsteen, K. *J. Am. Chem. Soc.* **1993**, *115*, 5294. (f) Trost, B.; Hashmi, A. S. K. *Angew. Chem.* **1993**, *105*, 1130; *Angew. Chem., Int. Ed. Engl.* **1993**, *32*, 1085.
- (12) The precatalyst mixture [RuCl₂(p-cymene)]₂/2N-heterocyclic carbene precursor/4C₂CO₃ also possesses enyne metathesis activity. (a) Semeril, D.; Bruneau, C.; Dixneuf, P. H. *Adv. Synth. Catal.* **2002**, *344*, 585. (b) Ackermann, L.; Bruneau, C.; Dixneuf, P. H. *Synlett* **2001**, 397. (c) Semeril, D.; Bruneau, C.; Dixneuf, P. H. *Helv. Chim. Acta* **2001**, *84*, 3335. The mechanism of catalysts without active carbene ligand is not investigated in this study.
- (13) Trnka, T. M.; Day, M. W.; Grubbs, R. H. *Organometallics* **2001**, *20*, 3845.
- (14) Mori, M.; Sakakibara, N.; Kinoshita, A. *J. Org. Chem.* **1998**, *63*, 6082. In its footnote 7, the authors state that a faster [2 + 2] cycloaddition of the alkene compared to the alkyne substrate would also be in accordance with the experimental observations.
- (15) (a) Becke, A. D. *J. Chem. Phys.* **1993**, *98*, 5648. (b) Volko, S. H.; Wilk, L.; Nusair, M. *Can. J. Phys.* **1980**, *58*, 1200. (c) Lee, C.; Yang, W.; Parr, R. G. *Phys. Rev. B* **1988**, *37*, 785.
- (16) Jaguar 4.1, release 59; Schrödinger, Inc.: Portland, OR, 2001.

- (17) (a) Hehre, W. J.; Ditchfield, R. J.; Pople, A. *J. Chem. Phys.* **1972**, *56*, 2257. (b) Hariharan, P. C.; Pople, J. A. *Theor. Chim. Acta* **1973**, *28*, 213. (c) Frisch, M. J.; Pople, J. A.; Binkley, J. S. *J. Chem. Phys.* **1984**, *80*, 3265. (d) Krishnan, R.; Binkley, J. S.; Seeger, R.; Pople, J. A. *J. Chem. Phys.* **1980**, *72*, 650.
- (18) Hay, P. J.; Wadt, W. R. *J. Chem. Phys.* **1985**, *82*, 299.
- (19) Schaftenaar, G.; Noordik J. H. *J. Comput.-Aided Mol. Des.* **2000**, *14*, 123.
- (20) (a) Clark, T.; Chandrasekhar, J.; Spitznagel, G. W.; Schleyer, P. v. R. *J. Comput. Chem.* **1983**, *4*, 294. (b) McLean, A. D.; Chandler, G. S. *J. Chem. Phys.* **1980**, *72*, 5639.
- (21) (a) Cooper, J.; Ziegler, T. *Inorg. Chem.* **2002**, *41*, 6614. (b) Tobisch, S. J. *Am. Chem. Soc.* **2004**, *126*, 259. (c) Straub, B. F.; Gollub, C. *Chem. Eur. J.* **2004**, *10*, 3081.

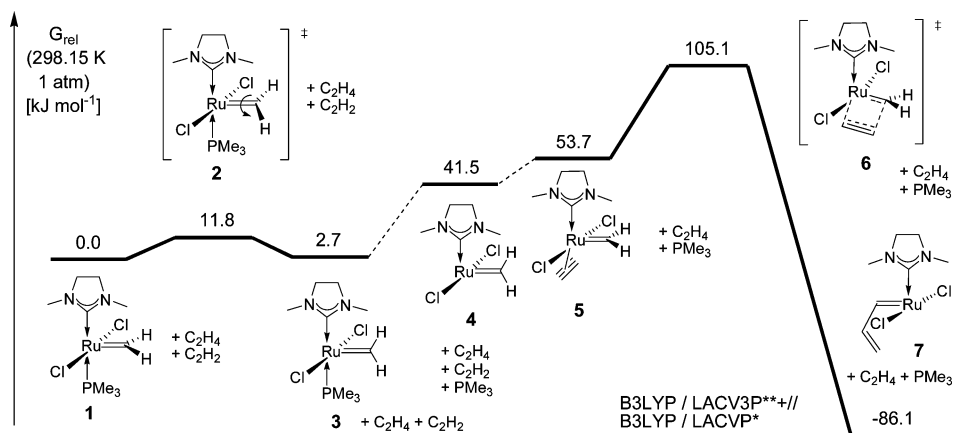


Figure 1. Energy diagram for ethyne insertion into a Ru=C bond in intermolecular enyne metathesis.

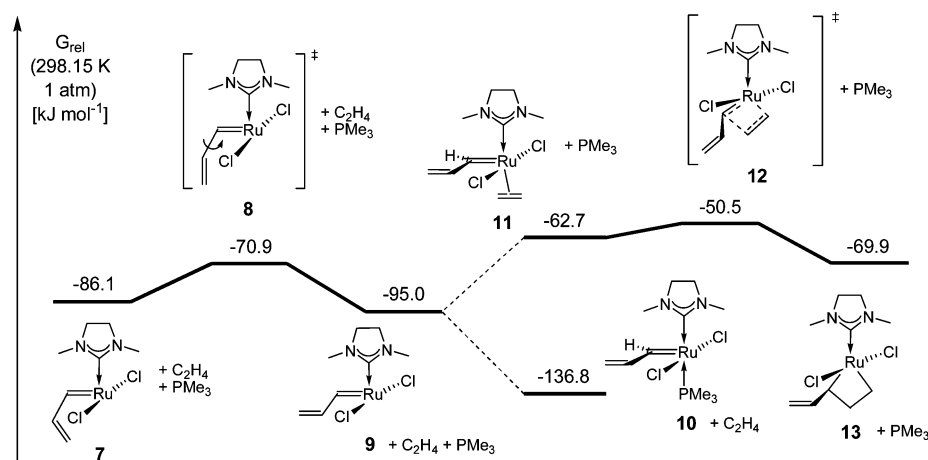


Figure 2. Energy diagram for vinyl group rotation and [2 + 2] cycloaddition of ethene and a vinylcarbene–ruthenium complex in intermolecular enyne metathesis.

of substrate substituents by appropriate choice of our model system. Our electronic core system is based on the model substrates ethene, ethyne, or hept-1-en-6-yne on one hand and on PMe_3 , CH_2 , and the *N*-heterocyclic carbene (“NHC”) spectator ligand derived from *N,N'*-dimethylimidazolidine as ligands at the ruthenium center on the other hand. Steric repulsion between the NHC mesityl substituents and substrate substituents of course influences significantly stabilities of intermediates and barriers within the catalytic cycle. It is our goal, however, to provide theoretical information about intrinsic electronic barriers without steric effects. Only by understanding of the basic mechanism can large steric effects in experimental enyne metathesis reactions be identified as what they are.

Content of the Study. The first part of this study (Figures 1–4) reports on the mechanism of the intermolecular enyne metathesis. Alkene metathesis (Figure 5), alkyne polymerization side reaction (Figure 6), relative orientation of alkene, alkyne, and carbene ligands (Figure 7), a nonproductive (“dead-end”) equilibrium (Figure 8), the regioselectivity issue (Schemes 3 and 4), as well as an alternative, highly disfavored pathway (Figure 9) are considered for a complete picture of the intermolecular title reaction. The influence of steric congestion on the stabilities of vinylcarbene coordination modes is presented in Scheme 5. The computed pathways of a first-generation Grubbs model system will be discussed only shortly in Table 1. In Scheme 6, an additional intermediate and transition state in the alkyne insertion sequence by a first-generation catalyst

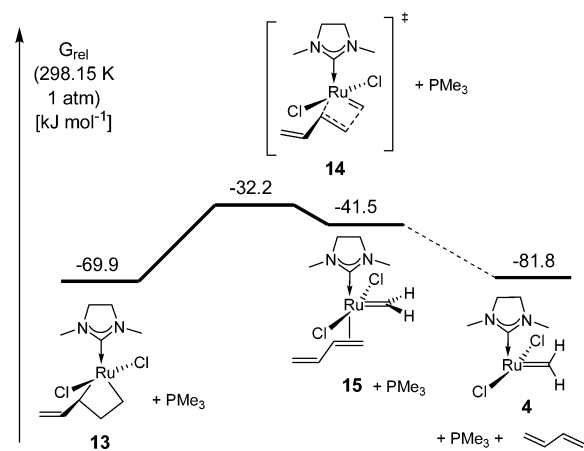


Figure 3. Energy diagram for [2 + 2] cycloreversion in intermolecular enyne metathesis.

model is shown. The relationship of the Dötz reaction and enyne metathesis is discussed in Scheme 7.

The second part of this study reports on the mechanism of the intramolecular enyne metathesis with second-generation Grubbs catalysts. Two pathways have been investigated: Alkene metathesis followed by alkyne insertion features a lower overall barrier (Figures 10–12). The influence of alkene substituents on the barrier for liberation of the diene product from ruthenium vinylcarbene complexes is presented in Table 2. Alkyne insertion followed by alkene metathesis is disfavored (Figures 13 and

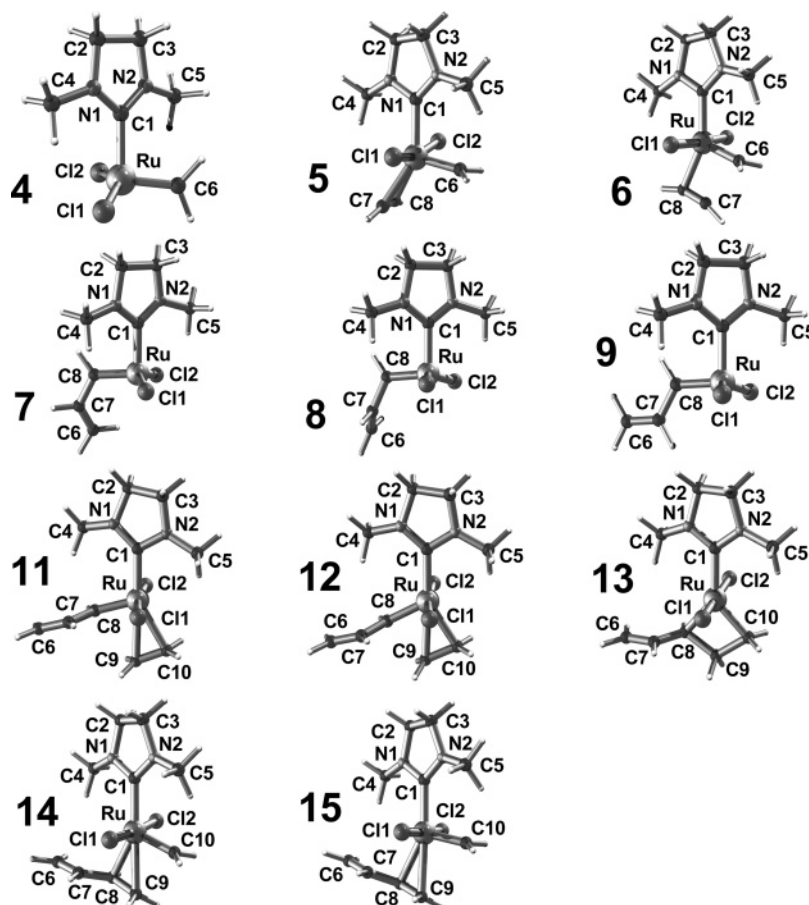


Figure 4. Ball-and-stick models of intermediates (4, 5, 7, 9, 11, 13, and 15) and transition states (6, 8, 12, and 14) of the computed catalytic cycle.

14). The latter pathway, however, can still be operative in some ring-opening metathesis–enyne metathesis reactions. General mechanistic proposals are finally summarized in Figure 15 for intermolecular enyne metathesis and in Figure 16 for intramolecular enyne metathesis.

Intermolecular Enyne Metathesis. First, we discuss the mechanistic pathway for the intermolecular enyne metathesis with a model complex for a second-generation Grubbs catalyst.²² The energies of the catalyst model **1** and the free substrates are taken as a reference for other energies and thus normalized to zero. The rotation of the methylene unit around the Ru=C axis in the almost degenerate structures **1** and **3** has a very low barrier via transition state **2** (Figure 1). Indeed, steric effects determine the orientation of the carbene fragment in experimental systems.²³

Grubbs catalysts are known to undergo dissociative ligand exchange.^{4d} After phosphane dissociation to the 14 valence electron complex **4**, ethyne coordinates to the ruthenium center *trans* to the NHC (*N*-heterocyclic carbene) spectator ligand. Experimentally, Grubbs et al. determined an overall activation barrier of $\Delta G^\ddagger = 96 \text{ kJ mol}^{-1}$ for phosphane dissociation in a second-generation PCy₃ ruthenium phenylcarbene complex.^{4e} The thermodynamic binding energy of the phosphane ligand in the model complex **1** is presumably underestimated. However, the number of molecules in the phosphane elimination process

remains constant, and the thermodynamic entropy gain is realized only after complete phosphane dissociation. The overestimation of entropic effects in the gas phase and the used level of theory might further contribute to the underestimation of the ruthenium bond strength. These effects will only have a secondary effect on a computed overall barrier, since the ruthenium coordination number is the same in the catalyst resting state and in the rate-limiting transition state: The coordination strength of ethyne is presumably equally underestimated. The binding energy of ethyne in complex **5** has a similar order of magnitude as the entropic contributions for this associative step. The insertion of the ethyne ligand into the ruthenium carbene unit features an overall Gibbs free activation energy of $\Delta G^\ddagger = 105.1 \text{ kJ mol}^{-1}$. The corresponding transition state **6** structurally resembles that of a [2 + 2] cycloaddition step. However, the ring strain associated with an sp²–sp² double bond in a hypothetical ruthenacyclobut-2-ene structure leads to the immediate rearrangement to the *cisoid*-vinylcarbene complex **7**. Overall, the ethyne insertion features a high barrier in the intermolecular enyne metathesis pathway. Nonetheless, the ethyne insertion is a highly exergonic process and represents the only irreversible step in the catalytic cycle. Remarkably, this slow insertion step via **6** with its high barrier is responsible for the release of the Gibbs free energy of the complete catalytic cycle.

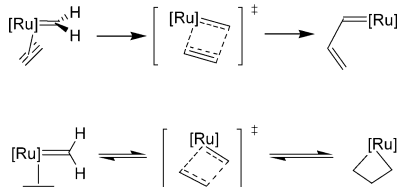
Ruthenacyclobut-2-enes in enyne metathesis were generally assumed as catalytic intermediates in analogy to the ruthenacyclobutane fragment in alkene metathesis.⁵ However, the

(22) Lippstreu, J. J., Diploma Thesis, Ludwig-Maximilians-Universität München, 2004.

(23) Fürstner, A.; Ackermann, L.; Gabor, B.; Goddard, R.; Lehmann, C. W.; Mynott, R.; Stelzer, F.; Thiel, O. R. *Chem. Eur. J.* **2001**, *7*, 3236.

increased ring strain due to two sp^2 carbon centers (ideal angle of 120°) instead of two sp^3 carbon centers (ideal angle of about 109°) destabilizes ruthenacyclobut-2-enes. Additionally, a productive, highly exothermic ring-opening rearrangement to vinylcarbene complexes enables unsaturated four-membered cyclic metal fragments to overcome their ring strain. As a result, *trans*-dichloro ruthenacyclobut-2-enes are only transient structures with a lifetime of a molecular vibration (Scheme 1).

Scheme 1. Mechanistic Difference of Alkyne Insertion into a Ruthenium Carbene Bond vs Alkene Cycloaddition with a Ruthenium Carbene



The facile rotation of the vinyl group in intermediate **7** via transition state **8** results in the central intermediate **9** (Figure 2). Because of its low ruthenium coordination number, phosphane as well as ethyne and ethene can coordinate to the metal center. PMe_3 addition yields complex **10**, an alternative catalyst resting state besides starting complex **1**. Ethyne coordination is the first step for alkyne oligomerization or polymerization (vide infra). Ethene addition to the *transoid*-vinylcarbene complex **9** yields intermediate **11**, which easily undergoes a reversible $[2 + 2]$ cycloaddition via transition state **12** to the 2-vinyl ruthenacyclobutane complex **13**.

In a $[2 + 2]$ cycloreversion reaction, the four-membered cycle of intermediate **13** yields either its precursor **11** or the butadiene complex **15** (Figure 3). Intermediate **15** is unstable, both with respect to its isomeric ethene complex **11** and ruthenacycle **13** as well as with respect to the dissociation of the diene ligand. The cycloreversion process from ruthenacycle **13** to butadiene complex **15** is characterized by a higher free activation energy than the cycloreversion from ruthenacycle **13** to ethene complex **11**. The electronic interaction of the vinyl substituent with a carbene ligand in model **11** is energetically more valuable than the mesomeric stabilization of the same vinyl group in the diene ligand in **15** by $\Delta G = 21.2 \text{ kJ mol}^{-1}$. Overall, the activation energy from phosphane complex **10** to the butadiene complex **15** amounts to $\Delta G^\ddagger = 104.6 \text{ kJ mol}^{-1}$. This barrier is almost identical to the overall barrier associated with the ethyne insertion step **6**. For intermolecular enyne metathesis, we thus can neither assign unequivocally the rate-limiting step (ethyne insertion **6** or cycloreversion **14**) nor the catalyst resting state (phosphane complexes **1** or **10**). Dissociation of buta-1,3-diene releases the reaction product and completes the catalytic cycle by formation of the active carbene complex **4**. The model reaction releases an overall free energy of $\Delta G = -123.3 \text{ kJ mol}^{-1}$.

Ball-and-stick models of all intermediates and transition states of the catalytic cycle are shown in Figure 4. The active carbene fragment switches from the “right” side of the ruthenium model complexes to the “left” side between structures **6** and **7** and back to the “right” side between structures **12** and **14**.

Alkene metathesis has already been investigated by several quantum-mechanical studies.⁵ Nonetheless, we wish to shortly present our results concerning this reaction for a better

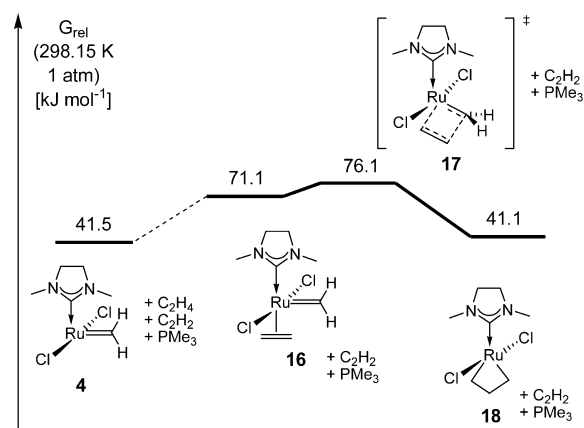


Figure 5. Energy diagram for alkene metathesis.

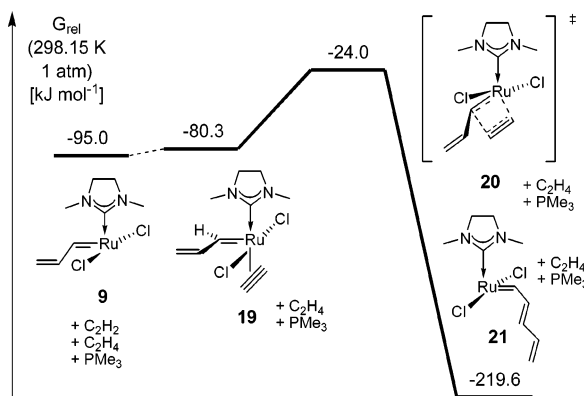


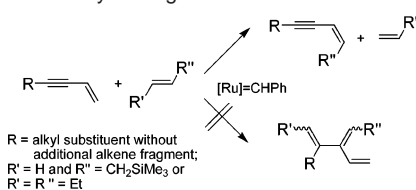
Figure 6. Energy diagram for ethyne insertion/alkyne polymerization as a possible side reaction in intermolecular enyne metathesis. An extra C_2H_2 has been added, and the Gibbs free energies have been normalized to be consistent with the energy data of Figures 1–5 and 7–9.

comparison of the structures, relative energies, and barriers with those of enyne metathesis at the same level of theory (Figure 5). The coordination strength of the ethene ligand in complex **16** is lower than that of ethyne in complex **5**. The cycloaddition step of ethene and ruthenium carbene, however, proceeds very easily.

So far, we have investigated the coordination of phosphane and ethene to the 14 valence electron fragment **9**. Coordination of ethyne to complex **19** opens the path for one step in an alkyne polymerization side reaction (Figure 6). The insertion of ethyne into the vinylcarbene ruthenium bond in transition state **20** results in an elongated unsaturated chain in the carbene ligand of complex **21**.

The overall barriers of ethyne insertion steps appear to be generally $20\text{--}30 \text{ kJ mol}^{-1}$ higher than ethene cycloaddition barriers. For example, this assumption holds true for the competing reactions at the vinylcarbene complex **9**. Ethene cycloaddition in structure **11** has an overall free Gibbs activation energy of $\Delta G^\ddagger = 86.3 \text{ kJ mol}^{-1}$, which is the energy difference between structure **10** plus ethene and transition state **12** plus phosphane. Ethyne insertion in complex **19** requires an overall free Gibbs activation energy of $\Delta G^\ddagger = 112.8 \text{ kJ mol}^{-1}$, which is the energy difference between structure **10** plus ethyne and transition state **20** plus phosphane.

The significantly higher barriers for alkyne insertions than for alkene metathesis reactions are not surprising. Hansen, Chang, and Lee et al. found that 1,3-enynes indeed display intermolecular alkene metathesis activity, thereby maintaining

Scheme 2. Intermolecular Alkene Metathesis with Conjugated Enynes Discovered by Chang et al.²⁴

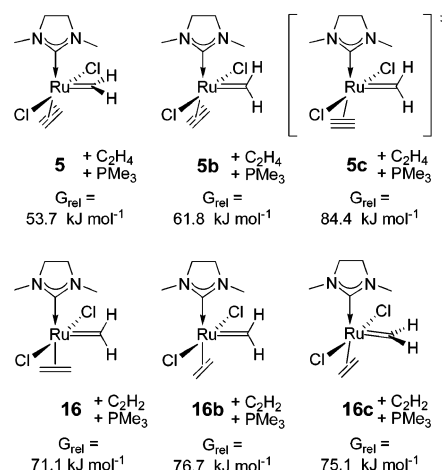
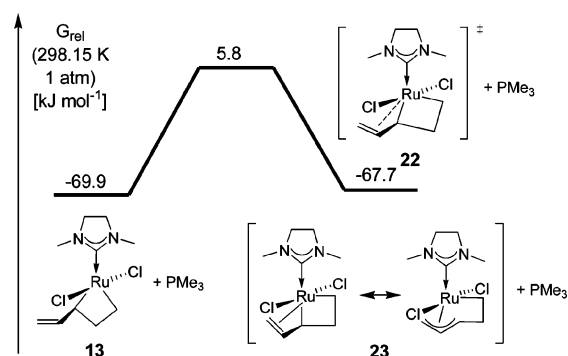
the C–C triple bond (Scheme 2).²⁴ Intramolecular enyne metathesis, however, is observed in 1,*n*-diene-3-yne (*n* = 10 or 15).^{24c} ¹H NMR investigations just recently provided evidence for fast alkene metathesis and comparatively slow enyne metathesis.²⁵

Why is the overall ethyne insertion barrier so high? Ethyne binds strongly to the ruthenium center, stronger than does ethene. However, the high intrinsic insertion barrier in the ethyne complex overcompensates this strong ethyne coordination. The high rotation barrier of the ethyne ligand around the ethyne ruthenium axis mainly contributes to the high insertion barrier (Figure 7). Stable rotameric minima in ethyne complexes feature an alkyne orientation orthogonal to the ruthenium carbene moiety. A parallel orientation is destabilized by more than 30 kJ mol⁻¹. However, such a parallel orientation is mandatory for the ethyne insertion to proceed. The analogous rotation of the ethene ligand is almost degenerate. Its most stable minimum structure features a parallel orientation of ethene ligand and ruthenium carbene fragment.

The alkyne coordination to the vinylcarbene complex **9** yields the aforementioned structure **19**. The ethyne insertion step can be regarded as the second step of an alkyne polymerization. The barrier is slightly higher than the cycloreversion and diene ligand formation via transition state **14**. The latter step necessitates prior ethene or alkene substrate coordination. Thus, a low ethene or alkene concentration increases the actual barrier for diene formation. This may lead to a lower product selectivity and to a higher content of alkyne polymerization side product. This selectivity problem may contribute to the successful implementation of the ethene atmosphere in “Mori’s conditions”. However, to the best of our knowledge, the conditions of formation, quantity, and identity of undesired oligomeric and polymeric side products in enyne metathesis have not been thoroughly investigated experimentally. Naturally, experimental efforts were directed toward optimizing reaction conditions to minimize such side reactions and to prevent polymer formation.

A further possible side reaction revealed itself as an unproductive equilibrium. The vinyl ruthenacyclobutane derivative **13** can rearrange to the similarly stable η^3 -allyl type complex **23** (Figure 8).²⁶ However, the barrier toward formation of complex **23** is higher than the barrier in the catalytic cycle for a productive diene formation from its precursor **13**. Thus, we do not expect structures such as η^3 -allyl complex **23** to play an important role in enyne metathesis.

Regioselectivity. Monosubstituted alkenes and alkynes always react to 1,3-substituted 1,3-dienes in intermolecular enyne

**Figure 7.** Relative Gibbs free energies of methylene, ethyne, and ethene rotamers.**Figure 8.** Energy diagram for an unproductive equilibrium in intermolecular enyne metathesis.

metathesis reactions. So far, we have only presented computational data for the enyne metathesis of ethene and ethyne substrate. Obviously, their reaction is unable to display regioselectivities. To identify the selectivity-determining step for substituted substrates, we used propene and propyne as model compounds. On the basis of these substrates, we investigated the barriers for two possible propyne insertion steps into a methylidene ruthenium bond and the analogous overall barriers for two possible propyne insertion steps into alkyldiene ruthenium bonds (Scheme 3). The methylcarbene complexes can be formed from the ruthenium methylidene model catalyst by propene cross metathesis.

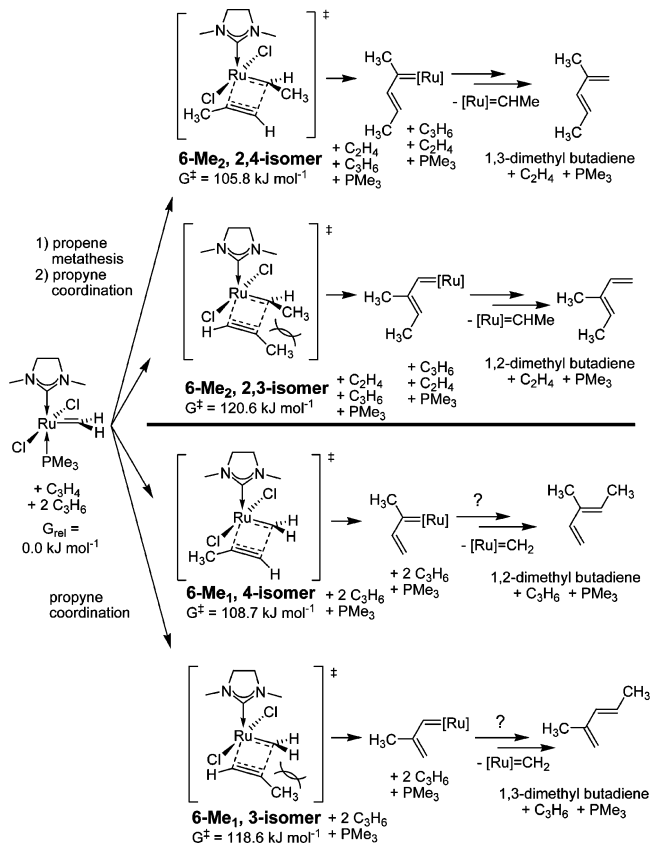
The computed overall Gibbs free energies of the transition states of propyne insertion into the ruthenium carbene bond differ considerably (Scheme 3). These differences can account for the observed 1,3-regioselectivity, since the most kinetically preferred model pathway leads to the 1,3-disubstituted product (row 1 in Scheme 3). However, an alternative methylidene pathway (row 3 in Scheme 3) is predicted to possess an overall Gibbs free activation energy only slightly higher by 2.9 kJ mol⁻¹. However, the respective total electronic energy barrier is more pronounced and amounts to 8.9 kJ mol⁻¹. On the basis of small barrier differences in our simplified model system, we can of course not generally rule out the participation of methylidene pathways. They might well be present in intermolecular enyne metathesis reactions under thermodynamic selectivity control. Subsequent cross metathesis of a monosubstituted diene intermediate with alkene substrate would also yield a 1,3-disubstituted diene product (Scheme 4).

(24) (a) Kang, B.; Lee, J. M.; Kwak, J.; Lee, Y. S.; Chang, S. *J. Org. Chem.* **2004**, *69*, 7661. (b) Hansen, E. C.; Lee, D. *Org. Lett.* **2004**, *6*, 2035. (c) Kang, B.; Kim, D.-h.; Do, Y.; Chang, S. *Org. Lett.* **2003**, *5*, 3041.

(25) Hansen, E. C.; Lee, D. *J. Am. Chem. Soc.* **2004**, *126*, 15074.

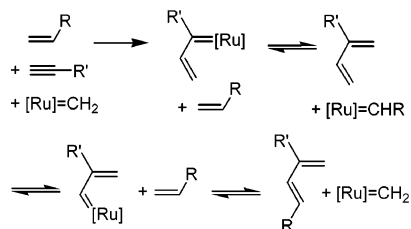
(26) We also found a further, more stable conformer with a relative free energy of G_{rel} = -72.1 kJ mol⁻¹.

Scheme 3. Comparison of Alkylidene (Rows 1 and 2) and Methylidene Pathways (Rows 3 and 4) for the Selectivity-Determining Alkyne Insertion Step^a



^a The most favored computed pathway (row 1) results in the experimentally observed 1,3-regioselectivity for intermolecular enyne metathesis.

Scheme 4. Thermodynamic Control of 1,3-Regioselectivity via a Ruthenium Methylidene Pathway



This mechanistic challenge can be illustrated by a literature example: In the enyne metathesis of internal silylated alkynes with terminal alkenes to trisubstituted dienes,^{8c} the steric repulsion in the alkyne-insertion transition state might perhaps be too strong for an alkylidene mechanism. This leads to the open question whether the isolated 2,3-disubstituted diene side product is an intermediate of a methylidene pathway under thermodynamic control, whether it is the cross metathesis product from the trisubstituted diene main product of a kinetically controlled reaction, or whether it is the product of an independent side reaction of the alkyne substrate with ethene that is generated by disproportionation of the terminal alkene substrate.

Despite the difficulty to evaluate the importance of thermodynamic control in 1,3-substitution selectivity, one general conclusion is evident from the theoretical data. In both the alkylidene pathways (rows 1 and 2 in Scheme 3) as well as in the methylidene pathways (rows 3 and 4), local steric repulsion

in the alkyne insertion step is the origin of kinetically controlled regioselectivity. The alkyne substituent suffers from steric crowding in the 2,3-isomer of the transition state **6-Me₂** (row 2) as well as in the 3-isomer of the transition state **6-Me₁** (row 4). In contrast, the propyne methyl group in the 2,4-isomer of **6-Me₂** (row 1) and the 4-isomer of **6-Me₁** (row 3) experience no comparable steric contact and thus lead to energetically preferred transition states. The C–C bond formation in the alkyne-insertion transition state already begins when the rehybridization processes of the carbene carbon and the alkyne carbon atoms are far from completion. Thus, the steric interaction between substituents is much stronger than anticipated for a four-membered cycle. In summary, the alkyne insertion is both the only irreversible step in the catalytic mechanism as well as the kinetically regioselectivity-determining step.

The insertion of a substituted alkyne into an alkylidene ruthenium bond will be elaborated again in the discussion on intramolecular enyne metathesis in the second part of this manuscript.

Intermolecular Alkyne Cycloaddition. As an alternative pathway for enyne metathesis, we investigated the intermolecular attack of ethyne at the 14 valence electron carbene complex **4** (Figure 9). The cyclopropanation-like high-energy transition state **24** is characterized by a predominant interaction of the carbene ligand with the ethyne substrate. Structure **24** collapses to the ruthenacyclobutene **25**. The barrier of this intermolecular C–C bond formation pathway is disfavored by almost $\Delta\Delta G^\ddagger = 100 \text{ kJ mol}^{-1}$, thus not competitive and not relevant for enyne metathesis. However, the rearrangement of the local minimum **25** via transition state **26** results in a more stable η^3 -vinylcarbene complex **27**. This structure can rearrange to or be formed via transition state **28** from *cisoid*-vinylcarbene complexes such as **29**. In our model system, vinylcarbene complexes (**7**, **9**, or **29**) are more stable than the isomeric η^3 -vinylcarbene complex **27**. In a more sterically engaged system, however, there is precedence for the η^3 -vinylcarbene coordination type at a ruthenium center.

Grubbs and co-workers isolated and structurally characterized a η^3 -vinylcarbene complex **30** (Scheme 5).¹³ This complex is reported to be thermally stable and unreactive in enyne metathesis reactions. At the first glance, there appears to be a contradiction between the high thermal stability of the experimental triphenyl derivative **30** and our theoretical prediction of a low thermodynamic stability of its sterically simplified model **27**. However, geometry optimization at same level of theory of structure **30** and its *transoid*-vinylcarbene isomer **31** resulted in a lower total electronic energy for the η^3 -complex **30**. Thus, the experimental relative stability of **30** is reproduced by our methodology. Apparently, complex **30** is stable only because of its steric congestion, which may also account for its catalytic inactivity.

First-Generation Catalyst Cycle. We also computed the mechanism of the enyne metathesis catalyzed by first-generation Grubbs catalysts. A second PMe_3 ligand was used as a simplified model ligand for the experimental PCy_3 . The PMe_3 model binds considerably stronger to ruthenium catalyst fragments than PCy_3 .⁵¹ The catalytic intermediates of the first-generation catalyst strongly resemble those of the second generation. Thus, we discuss the differences between the pathways of the two catalyst

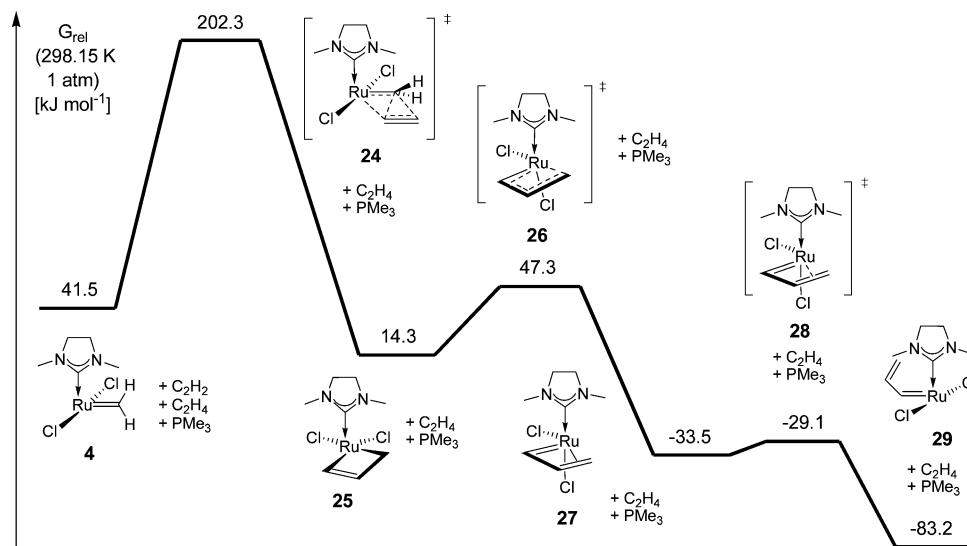
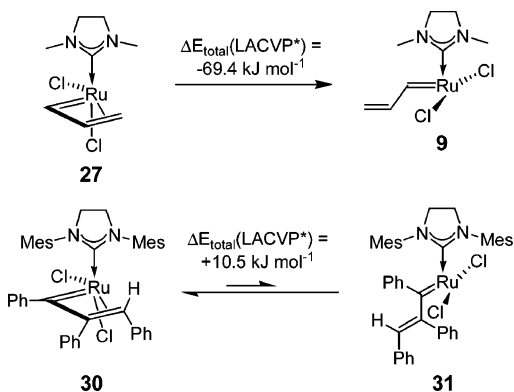


Figure 9. Energy diagram of a disfavored, high-barrier pathway for ethyne insertion in intermolecular enyne metathesis.

Scheme 5. Steric Stabilization of the *cis*-Dichloro η^3 -Vinylcarbene Ruthenium Complex **30**



systems only shortly. Table 1 contains the Gibbs free energy data of the phosphane analogues of the structures **1**–**29**.

The first-generation model catalyst features higher barriers for cycloaddition and insertion reactions than its second-generation analogue. This behavior originates from the first-generation catalysts general preference for higher coordination numbers and ruthenium(II) oxidation states. The ruthenacyclobutane phosphane complex **18** (1st) with its formal ruthenium oxidation state IV is relatively less stable than the second-generation NHC complex **18**. The smaller *trans* effect of a phosphane ligand compared to a heterocyclic carbene ligand results in higher phosphane dissociation energies. The experimentally observed lower barriers for PCy_3 dissociation in first-generation catalysts compared to second-generation catalysts^{4d,e} are a known artifact of the PMe_3 model.⁵¹ The main difference in the number of intermediates in the reaction path lies in the existence of a labile η^3 -vinylcarbene intermediate **32** (1st) (Scheme 6). It rapidly rearranges to the *cisoid*-vinylcarbene complex **7** (1st) with a computed barrier of less than 6 kJ mol^{-1} . A similar NHC complex **32** was neither found as a local minimum nor as a transition state due to the unfavorable *trans* coordination geometry of two strong σ -donor carbon atoms at the ruthenium center. We want to emphasize the structural difference of the isomeric η^3 -vinylcarbene complexes **27** (1st) and **32** (1st). The first isomer **27** (1st) features a *cis*-dichloro and *cis*-carbene-phosphane coordination pattern. The second

isomer **32** (1st) features a *trans*-dichloro and *trans*-carbene-phosphane coordination mode.

Mechanistic Analogies to the Dötz Reaction.

In the Dötz reaction, an alkyne ligand in a chromium carbene complex undergoes an intramolecular C–C-bond formation step.²⁷ As in ruthenium–carbene complex-catalyzed enyne metathesis, metallacyclobutenes were initially proposed as important intermediates. In the Dötz reaction, they were ruled out on the basis of theoretical considerations by the P. Hofmann group (Scheme 7).²⁸ There, a detailed discussion of the relative stabilities of metallacyclobut-2-enes versus η^3 -vinylcarbene complexes has already been presented.^{28b}

For an 18 valence electron alkyne chromium carbene complex, ligand coupling results in an 18 valence electron, closed-shell η^3 -vinylcarbene complex. The hypothetical chromacyclobut-2-ene is considered as an unstable, 16 valence electron, open-shell d^4 - ML_6 complex. Indeed, the experimentally observed regioselectivity of the Dötz reaction can be rationalized by the existence of η^3 -vinylcarbene intermediates but not by the existence of chromacyclobutenes.

The alkyne insertion steps of the enyne metathesis and the Dötz reaction resemble each other: Metallacyclobut-2-enes are not intermediates in either case. The unsaturated four-membered, d^4 - ML_5 -type 14 valence electron ruthenacycles, however, would be closed-shell species. Because of their high ring strain and the existence of a ring-opening pathway without barrier, *trans*-dichloro ruthenacyclobut-2-ene structures are not stable local minima but rearrange immediately to labile η^3 -vinylcarbene intermediates or directly to *cisoid*-vinylcarbene complexes.

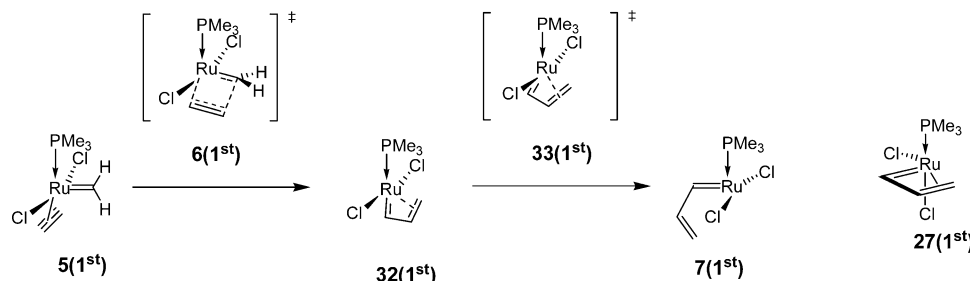
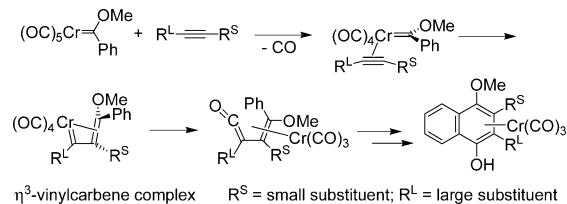
Intramolecular Enyne Metathesis. In the second part of our DFT study, we focus on the mechanism of intramolecular enyne metathesis (Scheme 8). Experimentally, this reaction typically proceeds under milder conditions than intermolecular enyne metathesis. From a mechanistic perspective, a linker between

- (27) (a) Dötz, K. H. *Angew. Chem.* **1975**, *87*, 672; *Angew. Chem., Int. Ed. Engl.* **1975**, *14*, 644. (b) Dötz, K. H. *Angew. Chem.* **1984**, *96*, 573; *Angew. Chem., Int. Ed. Engl.* **1984**, *23*, 587.
- (28) (a) Hofmann, P.; Hämmerle, M.; Unfried, G. *New J. Chem.* **1991**, *15*, 769. (b) Hofmann, P.; Hämmerle, M. *Angew. Chem.* **1989**, *101*, 940; *Angew. Chem., Int. Ed. Engl.* **1989**, *28*, 908. (c) Fischer, H.; Hofmann, P. *Organometallics* **1999**, *18*, 2590. (d) Gleichmann, M. M.; Dötz, K. H.; Hess, B. A. *J. Am. Chem. Soc.* **1996**, *118*, 10551.

Table 1. Relative Gibbs Free Energies of Intermediates and Transition States of First-Generation Model Complexes

model complex no.	G_{rel} (kJ mol ⁻¹)	model complex no.	G_{rel} (kJ mol ⁻¹)	model complex no.	G_{rel} (kJ mol ⁻¹)	model complex no.	G_{rel} (kJ mol ⁻¹)
1 (1 st)	0.0	33 (1 st) ^a	29.4	15 (1 st)	-46.2	22 (1 st)	18.3
2 (1 st)	2.6	7 (1 st)	-84.9	16 (1 st)	66.8	23 (1 st)	-68.7
3 (1 st)	-8.6	8 (1 st)	-68.6	16b (1 st)	69.3	24 (1 st)	231.6
4 (1 st)	43.3	9 (1 st)	-91.4	16c (1 st)	90.4	25 (1 st)	48.9
5 (1 st)	69.3	10 (1 st)	-136.6	17 (1 st)	99.1	26 (1 st)	91.2
5b (1 st)	55.9	11 (1 st)	-55.9	18 (1 st)	78.4	27 (1 st)	19.1
5c (1 st)	79.3	12 (1 st)	-23.5	19 (1 st)	-69.0	28 (1 st)	24.5
6 (1 st)	135.7	13 (1 st)	-31.9	20 (1 st)	5.4	29 (1 st)	-48.7
32 (1 st) ^a	23.7	14 (1 st)	-9.5	21 (1 st)	-214.4		

^a The additional structures **32**(1st) and **33**(1st) can be found chronologically correct between **6**(1st) and **7**(1st).

Scheme 6. Local Minima [**5**(1st), **32**(1st), and **7**(1st)] and Transition States [**6**(1st) and **33**(1st)] for Ethyne Insertion in First-Generation Ruthenium Carbene Complexes and Isomer **27**(1st)**Scheme 7.** Mechanism of the Dötz Reaction Proposed by the P. Hofmann Group²⁸

η^3 -vinylcarbene complex R^S = small substituent; R^L = large substituent

Scheme 8. Intramolecular Enyne Metathesis

the alkene and the alkyne fragment leads only to a subclass of the general reaction. We only consider second-generation catalysts due to their high intrinsic reactivity. We are aware that, with sterically demanding substrates, first-generation catalysts are often superior.²⁹ We used hept-1-en-6-yne as model substrate, where the alkene and alkyne moieties are part of the same molecule. Vinyl cycloalkenes are the product of the computed enyne metathesis pathway.

Entropic effects typically increase the rate (and decrease the barrier) of intramolecular reaction steps compared to their intermolecular analogues. In enyne metathesis, an unsaturated carbon-carbon substrate fragment should react more easily with the ruthenium carbene fragment in an intramolecular step. Two alternative pathways are possible: Primary alkene metathesis followed by intramolecular alkyne insertion is the first possibility. Alternatively, primary alkyne insertion can be followed by intramolecular alkene metathesis. In either case, the first

intermolecular reaction of the enyne substrate with the catalyst will have a strong effect on the rate of the second reaction, because this second step then must proceed intramolecularly. Therefore, we investigated both pathways for the enyne metathesis reaction of hept-1-en-6-yne to 1-vinylcyclopentene. From literature data and our computational investigation on the intermolecular enyne metathesis reaction (vide supra), a fast alkene metathesis sequence and a subsequent intramolecular alkyne insertion would be expected as the favored pathway. The computed mechanism of this pathway is discussed first.

Phosphane dissociation and alkene coordination at the second-generation model catalyst **1** lead to the isomeric complexes **34** and **35** (Figure 10). The alkyl substituent at the alkene substrate decreases the alkene's binding strength to the ruthenium center in the complexes **34** and **35** compared to the analogous ethene complex **16**. Nevertheless, the cycloaddition transition state **36** remains energetically accessible, yielding ruthenacyclobutane **37**. [2 + 2] Cycloreversion of structure **37** via structure **38** forms ethene complex **39**.

We did not investigate all possible diastereomeric pathways induced by the chiral information in the NHC ligand, because the staggering orientation of the NHC (CH₂)₂ fragment results in insignificant energetic changes. For example, the diastereomer of structure **37** is disfavored by only 1.4 kJ mol⁻¹.

The alkylcarbene complex **39** eliminates its ethene ligand, and may coordinate phosphane to structure **40** in an unproductive equilibrium. Phosphane redissociation easily leads back to the 14 valence electron complex **41** (Figure 11). Intramolecular coordination of the terminal alkyne triple bond to the ruthenium carbene complex **41** results in the 16 valence electron complex **42**. Here, the electronic binding energy compensates for the unfavorable loss of rotational degrees of freedom of the carbene side chain. The insertion of the alkyne ligand into the ruthenium carbene bond in transition state **43** proceeds with a predicted Gibbs free activation energy of 52.9 kJ mol⁻¹. This order of magnitude of 50–55 kJ mol⁻¹ is typical for alkyne insertion

(29) Randl, S.; Lucas, N.; Connon, S. J.; Blechert, S. *Adv. Synth. Catal.* **2002**, *344*, 631.

(30) Louie, J.; Grubbs, R. H. *Organometallics* **2002**, *21*, 2153.

(31) Fischer, E. O.; Maasböl, A. *Angew. Chem.* **1964**, *76*, 645; *Angew. Chem., Int. Ed. Engl.* **1964**, *3*, 580.

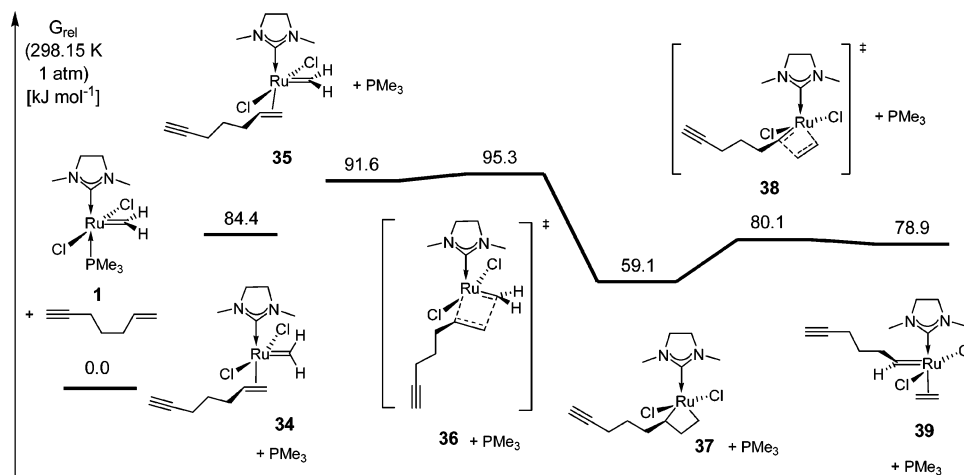


Figure 10. Energy diagram for the primary alkene metathesis sequence in intramolecular enyne metathesis.

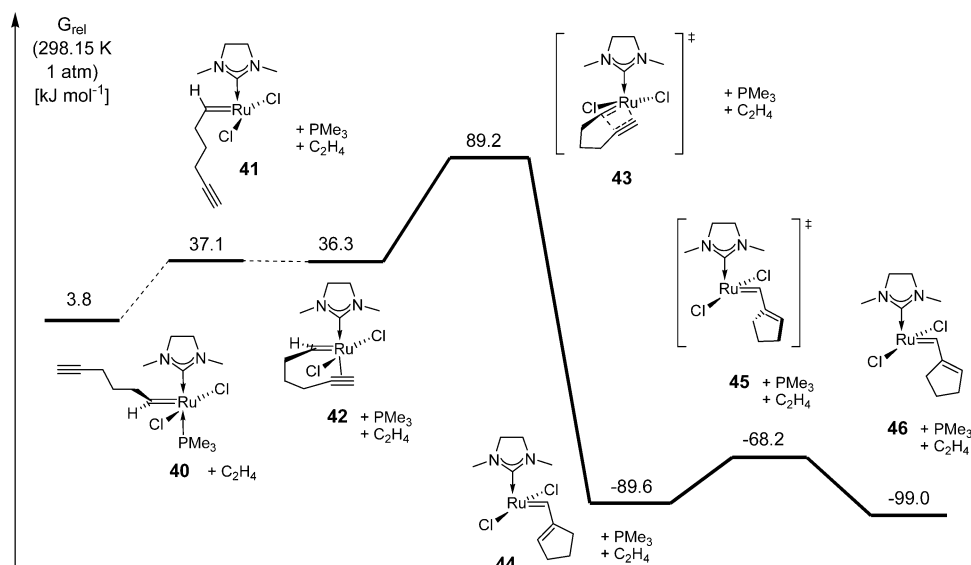


Figure 11. Energy diagram for the alkyne insertion sequence in intramolecular enyne metathesis.

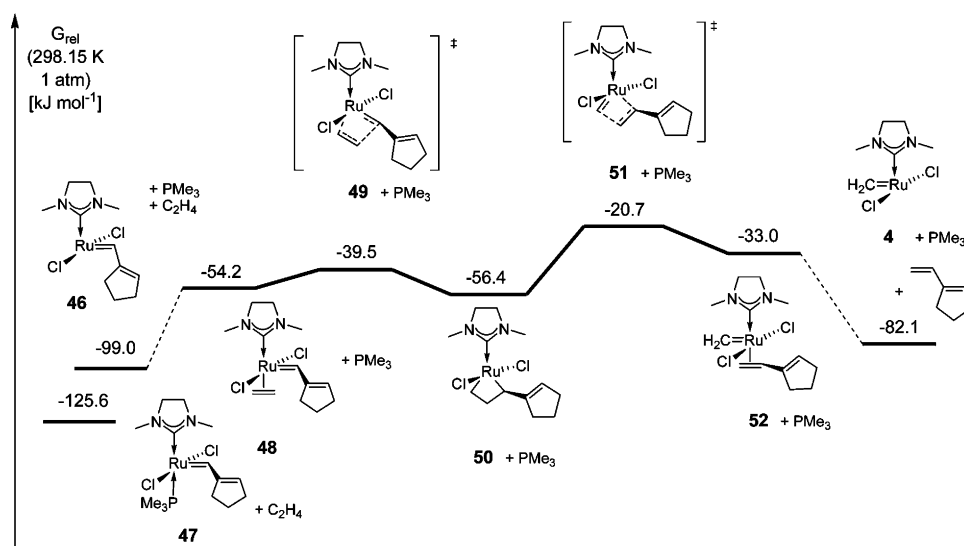


Figure 12. Energy diagram for the final ethene coordination and alkene metathesis in intramolecular enyne metathesis.

steps, since other computed alkyne insertion barriers reveal very similar values (see Figures 1 and 6 and *vide infra* Figure 13). The overall barrier of 85.4 kJ mol⁻¹ for alkyne insertion

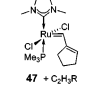
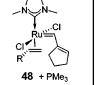
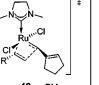
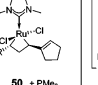
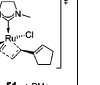
associated with transition state **43**, however, is smaller than in the previous examples (115.1, 105.1, and 112.8 kJ mol⁻¹). For overall insertion barriers, the Gibbs free-energy difference

between phosphane complex and ethyne insertion transition state is considered, respectively. The obvious origin for the decrease of the overall insertion barrier for step **43** is the entropically favored intramolecular phosphane ligand replacement by the alkyne side chain in structures **40–42**. In alkyne complexes **5**, **19**, and **53** (vide infra), the alkyne ligand replaces intermolecularly the phosphane ligand. As a consequence, the almost constant intrinsic activation energy is added to the low Gibbs free energy of alkyne carbene complex **42**, resulting in a low overall insertion barrier. The subsequent formation of the *cisoid*-cyclopentenylcarbene complex **44** is highly exergonic and thus irreversible. In analogy to the intermolecular pathway, the Gibbs free reaction enthalpy of the whole catalytic cycle is released in the alkyne insertion step. Rotation around the partial carbon–carbon double bond via **45** yields the slightly more stable *transoid* complex **46**.

The 14 valence electron complex **46** binds a phosphane ligand, yielding the catalyst resting state **47** (Figure 12). Of course, we cannot rule out that phosphane coordination already occurs at *cisoid* structures and rearrangement to *transoid* complexes takes place in a ruthenium phosphane complex. However, this detail is irrelevant for the understanding of the reaction. The chronological order of partial double-bond rotation vs phosphane coordination presumably depends on the phosphane concentration. After these two steps, ethene association to the unsaturated complex **46** opens the path for a [2 + 2] cycloaddition step from ethene complex **48** via transition state **49** to the four-membered ruthenacycle **50**. Subsequently, the [2 + 2] cycloreversion results in a diene methylene complex **52**. Again, this last cycloreversion step is rate limiting. As presented in Figure 3, a vinyl or in this case cyclopentenyl substituent has a stabilizing effect on a carbene fragment but destabilizes the binding of an alkene ligand to the ruthenium fragment. Thus, the diene carbene complex **52** is less stable than its ethene cyclopentenylcarbene isomer **48**. Since the cycloaddition/cycloreversion transition states are located 5–15 kJ mol⁻¹ above respective alkene carbene model complexes, the corresponding transition state **51** has consequently a higher Gibbs free energy than the isomeric transition state **49**. The catalyst resting state **47** and transition-state model **51** lead to a predicted overall Gibbs free activation energy of $\Delta G^\ddagger = 104.9$ kJ mol⁻¹. This value is also the overall barrier for the complete catalytic cycle. Dissociation of the diene ligand finally yields the active ruthenium complex **4**, awaiting new enyne substrate for the next catalytic turnover.

The formation of the 1-vinyl cyclopentene model product releases an overall free reaction energy of $\Delta G = -123.6$ kJ mol⁻¹. The almost identical free reaction energies for the hept-1-en-6-yne substrate on one hand and for ethene and ethyne on the other hand originate from the compensation of the favored entropic contribution $T\Delta S$ of an intramolecular addition and the smaller reaction enthalpy ΔH of the monosubstituted multiple bond systems in the intramolecular hept-1-en-6-yne substrate. The same line of argumentation also holds true for the almost identical computed overall Gibbs free reaction enthalpies of about 105 kJ mol⁻¹ for both the intermolecular (Figures 1 to 3) and for the intramolecular enyne model reaction (Figures 10–12). Substituted substrate models would increase the overall barriers in intermolecular enyne metathesis compared to the ethene/ethyne system.

Table 2. Relative Gibbs Free Energies of Selected Intermediates and Transition States in Intramolecular Enyne Metathesis

G_{rel} (298.15 K, 1 atm) [kJ mol ⁻¹] ^a					
R = H	-125.6	-54.2	-39.5	-56.4	-20.7
R = Me	-125.6	-45.1	-19.3	-39.8	-22.4
R = OMe	-125.6	-46.9	-15.8	-42.0	-36.9

^a Relative Gibbs free energies are normalized to that of complex **47** and the appropriate alkene, respectively. Relative Gibbs free energies of the rate-limiting steps are in bold numbers.

Substituent Influence in Diene Liberation.

Of course, Mori's conditions with their ethene atmosphere are mandatory for ethene coordination to complex **46**. Without ethene, the hept-1-en-6-yne substrate would have to coordinate to complex **46**, undergo the cycloaddition/cycloreversion sequence, and release the diene product. We thus investigated the influence of alkene substituents R on the barriers of this particular sequence. Propene was used as the simplest terminal aliphatic alkene (R = Me), similar to the hept-1-en-6-yne substrate. Methyl vinyl ether is an example for an extremely electron-rich alkene (R = OMe). The relative Gibbs free energies presented in Table 2 clearly suggest that more and stronger electron-donating substituents R at the alkene lead to a weaker alkene coordination in complexes **48–R** and to thermodynamically less stable ruthenacyclobutanes **50–R**. The cycloaddition steps via transition states **49–R** increase dramatically both in overall barriers as well as energetically relative to the respective alkene complexes. In contrast, the overall cycloreversion barrier via **51–R** is highest for the formation of a methylene complex **52** (with R = H). As a consequence, the identity of the rate-determining step changes from cycloreversion in the ethene-derived mechanism to cycloaddition in the vinyl ether-derived sequence. For a terminal alkene such as propene, cycloaddition **49–R** and cycloreversion **51–R** have very similar barriers, almost identical to that of the cycloreversion **51** of the ethene-derived ruthenacycle **50** (R = H). The experimental rate-enhancing effect of ethene is predicted to have no distinct electronic origin, but is based on a constantly high ethene concentration. Under ethene-free conditions, the reaction rate would decrease proportional to the alkene substrate concentration. Driving an enyne metathesis reaction to completion with stoichiometrically employed substrates and under ethene-free conditions would thus be almost impossible.¹⁴

Alternative Intramolecular Catalytic Cycle.

The alternative mechanistic pathway of intramolecular enyne metathesis is characterized by a primary enyne insertion followed by alkene metathesis of the substrate. This sequence features a higher overall barrier for enynes with a noncyclic alkene fragment. The dissociative phosphane versus alkyne ligand exchange yields complex **53** (Figure 13). The irreversible alkyne insertion is the rate-limiting step **54**. An overall Gibbs free activation energy of 115.1 kJ mol⁻¹ is already significantly higher than the predicted overall barrier of 104.9 kJ mol⁻¹ for the favored pathway in Figures 10–12 with a primary alkene metathesis sequence. Nevertheless, we continued to complete the second, high-energy catalytic cycle. Rotation of the vinyl substituent from *cisoid* complex **55** via transition state **56** yields the *transoid* complex **57**. Phosphane addition results in the 16 valence electron complex **58**. Intramolecular binding of the terminal vinyl fragment yields complex **59**.

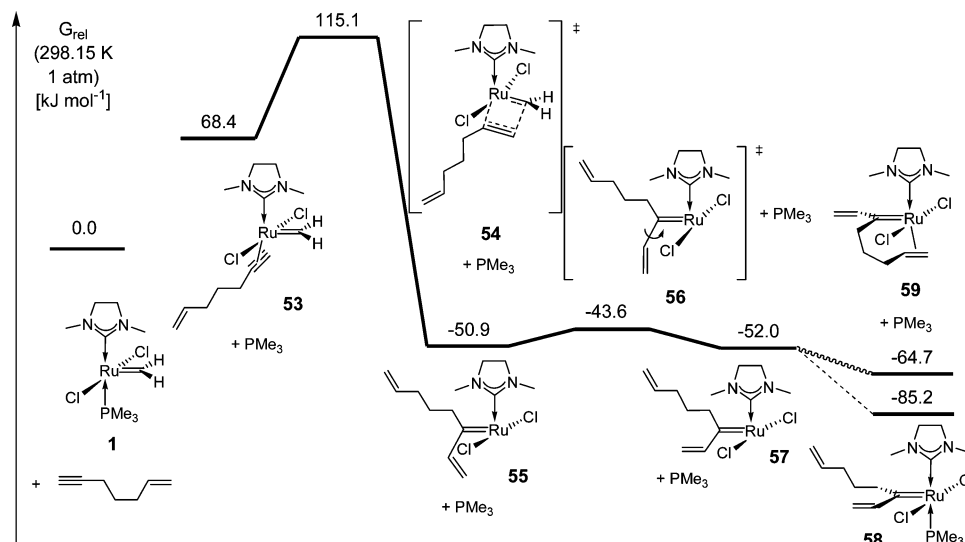


Figure 13. Energy diagram for the disfavored pathway of intramolecular enyne metathesis, comprising initial alkyne insertion.

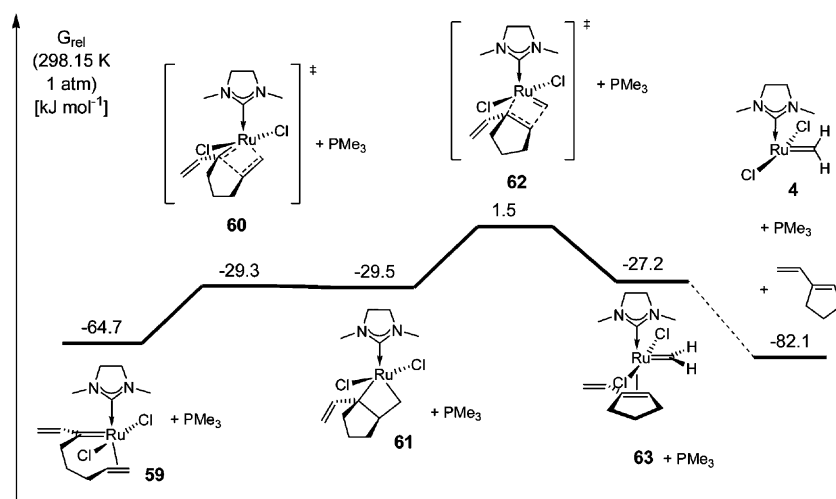


Figure 14. Energy diagram for the disfavored pathway of intramolecular enyne metathesis, comprising final alkene metathesis.

Upon cycloaddition via transition state **60**, the 6-ruthenabicyclo[3.2.0]heptane derivative **61** is formed (Figure 14). The latter yields the diene complex **63** via the cycloreversion transition state **62**. An overall barrier of $\Delta G^\ddagger = 86.7 \text{ kJ mol}^{-1}$ between the cycloreversion step **62** and phosphane complex **58** is lower than the overall barrier of $\Delta G^\ddagger = 115.1 \text{ kJ mol}^{-1}$ for the alkyne insertion **54** in the same mechanistic pathway (Figure 13). In this second pathway, ethene is neither produced nor consumed in any of the investigated steps. The experimental rate enhancement of enyne metathesis reactions in an ethene atmosphere is thus incompatible with the second mechanistic scenario.

In summary, the first, favored intramolecular mechanism (Figures 10–12) has a rate-limiting cycloreversion step. The second, disfavored, hypothetical pathway (Figures 13 and 14) is characterized by a rate-limiting intermolecular alkyne insertion step. The “strategy” of the intramolecular enyne reaction mechanism for achieving a minimal overall barrier is to make the intrinsically most difficult step, the alkyne insertion, an intramolecular, entropically favored rearrangement.

Large Ring-Closing Enyne Metathesis.

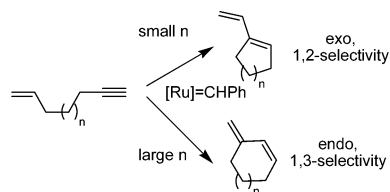
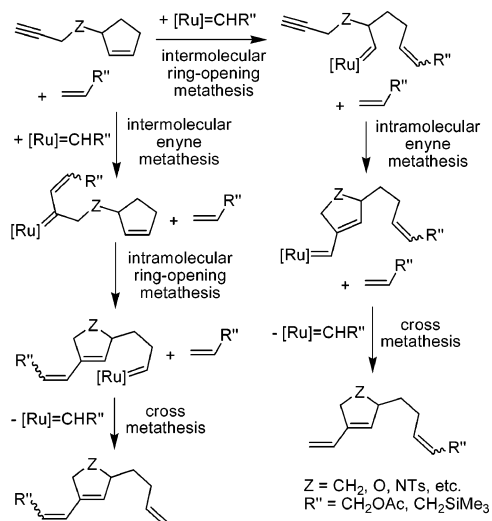
In intramolecular (ring-closing) enyne metathesis, an extended alkane linker between alkene and alkyne fragment leads to cyclic 1,3-disubstituted diene products.²⁵ With such a sufficiently large

linker, the 2,4 isomer of a transition state analogue of **43** is more favored than its 2,3 isomer (see Figure 11 and Scheme 3). Thus, our computational data supports the mechanistic proposal of E. C. Hansen and D. Lee that the “alkene-initiation route can explain the outcome of the RCEYM reaction”...“more effectively than the alkyne-initiation route.” Because of the steric repulsion in medium-sized ring systems, it is reasonable that a reported intermolecular enyne metathesis with ethene is faster than intramolecular enyne metathesis.

Domino Ring-Opening Cross Metathesis: Intramolecular Enyne Metathesis.

The reaction of monosubstituted alkenes with cycloalkenes containing an alkyne side chain has found considerable interest in recent years.²⁹ Depending on the substrates, evidence for primary cross metathesis or primary enyne metathesis has been presented (Scheme 10).²

The difference of these domino-reaction sequences compared to the enyne metathesis pathways outlined above is the entropic destabilization of the primary alkene metathesis sequence. In the domino RCM enyne metathesis, the fast and reversible ring-opening step combines two molecules (substituted cycloalkene and ruthenium carbene) into one single molecule. In the first step of “normal” intramolecular enyne metathesis, the enyne

Scheme 9. Exo/1,2- vs Endo/1,3-Selectivity Investigated by Lee et al.²⁵**Scheme 10.** Two Alternative Pathways of Domino Ring-Opening Cross Metathesis–Intramolecular Enyne Metathesis

substrate also coordinates at the ruthenium catalyst, but then an alkene (e.g., ethene) is released in an entropically favored dissociation step. For the domino reaction, the intramolecular alkyne-insertion step would take place from a higher Gibbs free energy level. Thus, an alternative primary intermolecular alkyne insertion with subsequent ring opening becomes competitive. As a consequence, the substitution pattern of the substrates can determine the order of alkyne insertion and cycloalkene ring opening by cross metathesis, and both mechanisms are energetically competitive. For domino ring-opening cross metathesis–intramolecular enyne metathesis reactions, we thus agree with Blechert et al. that the existence of alternative mechanisms “highlights the inherent dangers of making assumptions regarding the general mechanism of this relatively young reaction”.²

Mori's Conditions.

The Mori group discovered that an ethene atmosphere has a strong rate-enhancing effect on intramolecular enyne metathesis reactions catalyzed by Grubbs carbene complexes.¹⁴

We would like to point out three reasons for these experimental observations.

(1) Ethene has a protective effect toward ruthenium ethoxy-carbene complexes.^{8d,30} However, we have not quantum chemically investigated decomposition pathways for this rather special Fischer-type³¹ carbene complex.

(2) Generally, ethene is predicted to inhibit alkyne polymerization side reactions due to competitive alkyne ligand replacement by ethene (see Figures 6 and 15).

(3) The rate-enhancing effect of an ethene atmosphere can be explained with the mechanisms predicted in this study. Ethene or the alkene substrate, respectively, displace phosphane from the vinylcarbene catalyst resting state and are subsequently incorporated in a ruthenacyclobutane. Thus, the rate-limiting

step of the overall catalytic cycle is structurally different for Mori's condition and for ethene-free reactions. With terminal alkene substrates, however, their barriers are almost identical (Table 2). The difference in reaction rates between Mori's conditions and direct, ethene-free reactions originates from the significantly higher overall alkene concentration that are present under Mori's conditions.

From our proposed mechanistic scenario, we generally expect a first-order dependence of the reaction rate on the ethene/alkene concentration and on the catalyst concentration. A first-order dependence on the alkyne concentration and a zeroth-order dependence on the ethene concentration would indicate a mechanism with a rate-limiting alkyne-insertion step and a 16 valence electron phosphane ruthenium methylene (or, e.g., phenylcarbene) complex as catalyst resting state. The intermolecular reactions of alkynes with cyclic alkenes developed by the S. T. Diver group might also be insensitive toward ethene,^{8c,d} since the alkene fragment is already present in the vinylcarbene intermediate.

Conclusions

Eight general conclusions result from our quantum-chemical model calculations of the enyne metathesis reaction.

(1) Ruthenacyclobut-2-ene derivatives are no intermediates

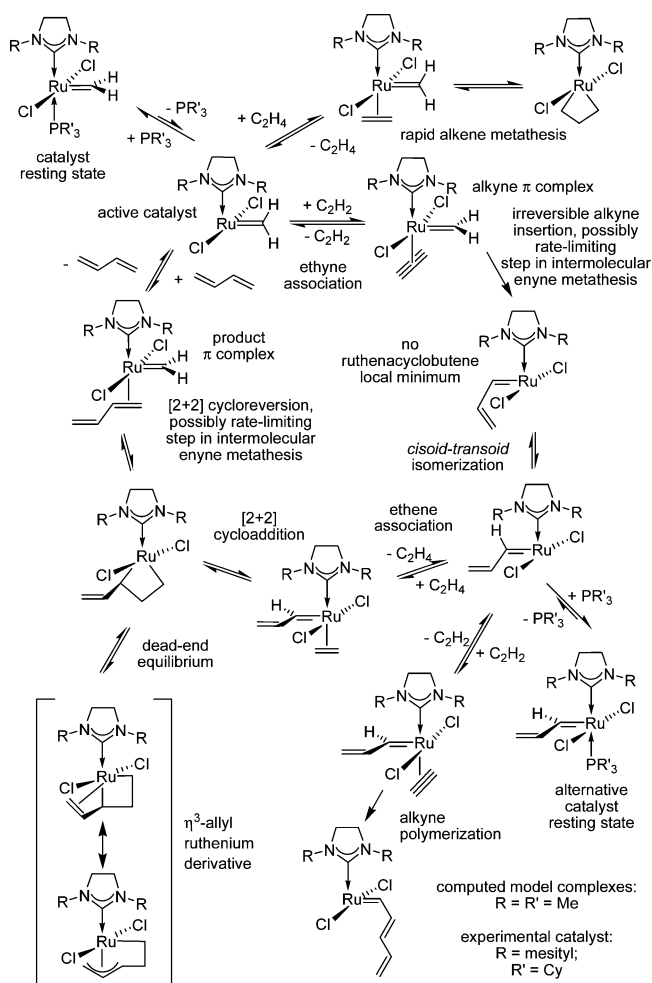


Figure 15. Catalytic cycle of intermolecular enyne metathesis, including pre-equilibria, a side reaction, and an unproductive equilibrium. Under ethene-free conditions and with electron-rich alkene substrates, their cycloaddition to the vinylcarbene complex may be rate limiting.

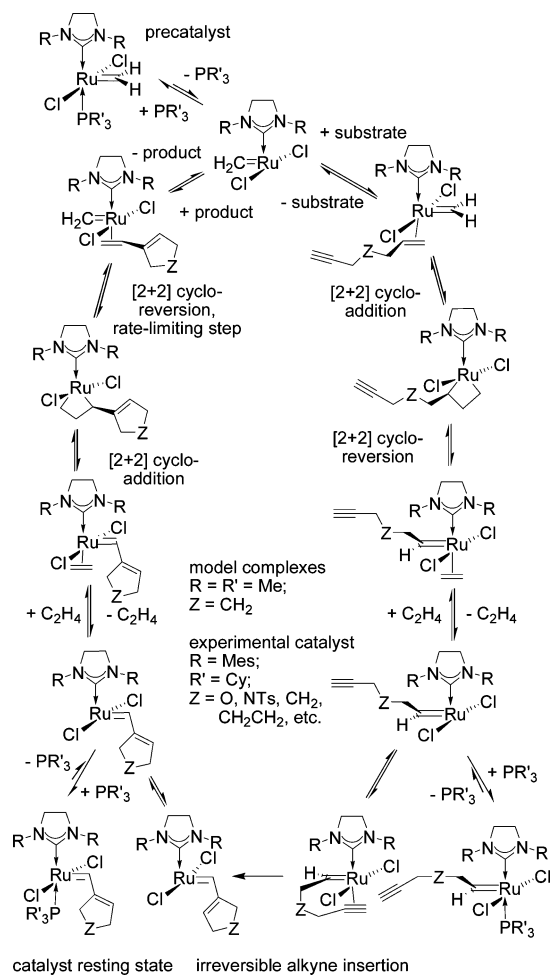


Figure 16. Catalytic cycle of intramolecular enyne metathesis, including phosphane coordination equilibria. Under ethene-free conditions and with electron-rich alkene substrates, their cycloaddition to the vinylcarbene complex is rate limiting. The mechanism in this figure does not necessarily apply to ring-opening metathesis–enyne metathesis reactions.

in the catalytic cycle, and even their η^3 -vinylcarbene valence isomers are at most labile and short-lived catalytic intermediates.

(2) Alkynes bind stronger to 14 valence electron catalyst fragments than alkenes with comparable substitution pattern.

(3) Alkyne insertion steps into ruthenium carbon double bonds display significantly higher intrinsic barriers than alkene plus ruthenium carbene [2 + 2] cycloaddition reactions. As a consequence, the overall barrier for alkyne insertion is about 20–30 kJ mol⁻¹ higher than the overall barrier for a comparable alkene metathesis sequence.

(4) Alkyne insertion into a ruthenium carbene bond is the only irreversible step in the catalytic cycle. Furthermore, it is the kinetically regioselectivity-determining step responsible for the formation of 1,3-disubstituted 1,3-dienes in intermolecular enyne metathesis.

(5) In intermolecular enyne metathesis, either the alkyne insertion or the cycloreversion to the diene product complex can be rate limiting (Figure 15). On the basis of the experimental data in the literature,⁶ we assume that rate-limiting cycloreversion is more common or maybe even generally operative.

(6) In intramolecular enyne metathesis under Mori's conditions, the cycloreversion of 2-vinyl-1-ruthenacyclobutanes to the diene product complex is rate limiting (Figure 16). With terminal alkene substrates under ethene-free conditions, the rate-limiting steps cycloaddition of the alkene to the vinylcarbene complex and the subsequent cycloreversion feature similar overall barriers.

(7) Added ethene is incorporated instead of the alkene substrate in the diene product formation. This leads to a structurally different rate-limiting step, however, with a similar Gibbs free barrier as for similar alkene substrate concentrations. The rate enhancement under Mori's conditions mainly originates from the constantly high concentration of ethene particularly in diluted substrate solutions and after high alkene substrate conversion.

(8) A high ethene concentration facilitates the competitive displacement of alkyne ligands by ethene and may thus suppress alkyne insertion into vinylcarbene ruthenium bonds, which may lead to alkyne polymerization side products.

We have investigated complete catalytic hypersurfaces neither with substrates with strongly electron-withdrawing nor with electron-donating substituents (see, however, Table 2). Thus, the influence of such substituents on overall catalytic cycles cannot be reliably derived from this study.

The complete catalytic cycles for intermolecular and intramolecular enyne metathesis are summarized in Figures 15 and 16. The proposed intermolecular mechanism has many similarities to previously proposed detailed catalytic cycles^{6a,8b} but also some distinct differences. We underline the comment of Diver and Giessert^{6a} that, although in the mechanisms proposed in the literature “all steps are written as reversible,”...“reversibility has not been established, particularly in the sequence” alkyne complex (to ruthenacyclobutene) to vinylcarbene complex.

Of course, steric effects between bulky enyne substrates and the spectator ligands of the Grubbs catalyst can overcome electronic effects. Second-generation catalysts are inactive toward sterically demanding enyne substrates so that first-generation catalysts must be employed.²⁹ For such reactions, this study serves as a tool to identify and quantify significant steric effects. This investigation may also be employed as a map for further studies. For the large majority of enyne metathesis reactions in the literature, the results in this manuscript shed some more light on the effects of substrate, ligands, and ethene on rate and selectivities.

Acknowledgment. A fellowship of the Fonds der Chemischen Industrie to B.F.S. and generous support from the LMU Munich and Prof. Herbert Mayr is gratefully acknowledged.

Supporting Information Available: Energy data, Cartesian coordinates of all structures, detailed basis set and effective core potential information. This material is available free of charge via the Internet at <http://pubs.acs.org>.

JA042622G